JOURNAL OF THEORETICAL AND APPLIED MECHANICS
62, 2, pp. 231-240, Warsaw 2024
https://doi.org/10.15632/jtam-pl/185163

ANALYSIS OF THE INFLUENCE OF GEOMETRICAL IMPERFECTIONS ON THE EQUIVALENT LOAD STABILIZING ROOF TRUSS WITH LATERAL BRACING SYSTEM[1]

Marcin Krajewski
Gdansk University of Technology, Faculty of Civil and Environmental Engineering, Gdansk, Poland
e-mail: markraje@pg.edu.pl

The paper is focused on the numerical analysis of the stability and load bearing capacity of a flat steel truss. The structure is supported by elastic lateral braces. The translational and rotational brace stiffness are taken into account. The linear buckling analysis is performed for the beam and shell model of the truss. The nonlinear static analysis is conducted for the structure initial geometric imperfections. As a result, the buckling and limit load depending on brace stiffness has been obtained. The reactions in elastic braces are compared to stabilizing forces calculated on the basis of actual code requirements.

Keywords: truss, elastic braces, imperfection, stabilizing load

1. Introduction

Flat trusses are often designed as roof girders in large span steel halls. The characteristic feature for that type of constructions is high stiffness and load bearing capacity but only in their plane. In order to stabilize lattice structures in the roof plane, a bracing system is required (e.g. roof cross and longitudinal braces). In many cases, the braces are designed to carry out the horizontal wind loading but also to stabilize the whole roof.

In many cases, during the design process, it is assumed that the braces are rigid. On this basis, the buckling length of the compressed truss chord (out of plane) is calculated as a distance between lateral supports. The stability of trusses braced by elastic supports was considered by Iwicki (2007, 2010). The experimental tests subjected to gravity loading performed for a steel truss stiffened by elastic side supports were carried out by Jankowska-Sandberg and Kołodziej (2013) and also by Krajewski (2021). The influence of brace rotational stiffness (located at the top chord) on the truss bearing capacity in the case of wind loading was studied by Biegus (2015). In this case, on the basis of analytical solutions, a significant impact of rotational stiffness of side supports on the truss bearing capacity was confirmed. The influence of initial geometric imperfections on the truss bearing capacity subjected to wind loading was also investigated by Krajewski and Iwicki (2016).

Rotational stiffness results from bending stiffness of the brace (e.g. purlin) and connection stiffness between the brace and the truss top chord

$$\frac{1}{k_{rot}} = \frac{1}{K_{roof}} + \frac{1}{K_{con}} \tag{1.1}$$

where: k_{rot} – rotational stiffness of the elastic side support, K_{roof} – bending stiffness of the brace, K_{con} – connection stiffness between the brace and the truss top chord.

The vertical load subjected to a truss with an initial imperfection (e.g. arch curvature of the top chord due to Eurocode 3) generates horizontal forces in side braces. Based on the

[1]Paper presented during PCM-CMM 2023, Gliwice, Poland

actual code requirements (PN-EN 1993-1-1, 2005), the stabilizing load for roof trusses can be determined. However, it is worth noting that the solutions presented in codes are referred to elements with pinned supports and subjected to constant compression along the length. Based on solutions presented by Czepiżak (2013), the iteration process related to determination of the equivalent stabilizing load (due to code) can be omitted. In this case, the stiffness of the roof cross bracing system has to be calculated. Further analytical modifications of this solution were presented by Krajewski (2021). In that case, horizontal stabilizing forces can be calculated if the brace translational stiffness k [kN/m] is known Eq. (1.2). Analytical solutions focused on the determination of those forces were also presented by Biegus and Czepiżak (2018, 2019) and Czepiżak and Biegus (2016). In that case, the structure with an initial imperfection in the form of arch curvature was considered. Furthermore, the influence of the normal force variation along the compressed truss chord was taken into account

$$q_d = \frac{8\left(e_o + \frac{L_{st}}{k} q_z\right) \sum_{i=1}^{m} N_{ed}}{L^2 - 8\frac{L_{st}}{k} \sum_{i=1} m N_{ed}} \qquad R_d = q_d L_{st} \tag{1.2}$$

where: q_d – equivalent stabilizing load, L_{st} – distance between side braces, e_o – imperfection amplitude, k – elastic brace, q_z – horizontal external loading, N_{ed} – normal force at the truss top chord, L – structure length, m – number of braced elements, R_d – stabilizing force.

The present study is devoted to stability and load bearing capacity analysis of a braced truss. A structure with elastic braces is considered. A constant or parabolic brace stiffness distribution along the truss length is taken into account. The influence of intermediate supports stiffness (translational k [kN/m] and rotational k_{rot} [kNm/deg]) on the buckling load is studied. Also, nonlinear static analysis is performed for the structure with initial imperfections. Moreover, stabilizing forces determined on the basis of code requirements are compared to numerical results.

2. Description of the truss

The analysis has been performed for a truss made of steel (S275). The structure length was equal to 18.0 m and hight was 0.7 m. The top chord consisted of RHS $120 \times 100 \times 4$ profiles and the bottom chord of RHS $100 \times 100 \times 4$. The V type of a diagonal system (RHS $50 \times 50 \times 3$) was considered (Fig. 1). The separate members were joined by means of welded connections. The similar structure stiffened by a trapezoidal sheet and subjected to the wind loading was previously studied by Biegus (2015). The structure was pinned at both ends. The possibility of rotation (twisting out of the truss plane) was blocked at marginal supports. The distance between elastic side supports was equal to 3.0 m (brace numbers from 1 to 5, Fig. 1). In this case, the translational and rotational (out of plane) support stiffness was considered.

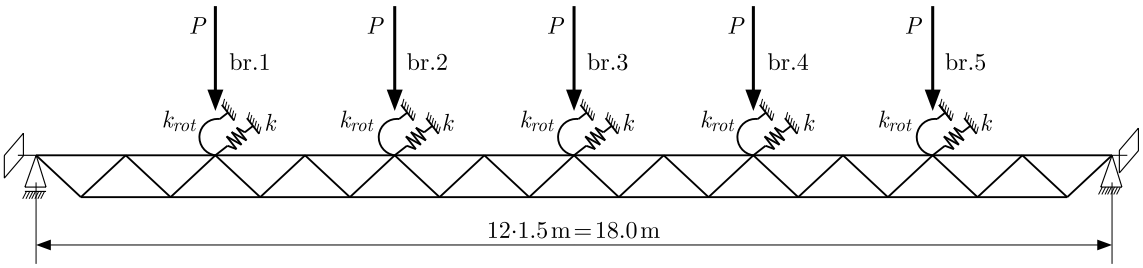

Fig. 1. The static schema

The finite element method was used to conduct analysis for the spatial beam and shell models of the truss. The numerical analysis were performed by means of Femap with NX Nastran (2009).

About 42 000 4-node and 3-node shell elements (QUAD4, with six degrees of freedom at node) were used (Fig. 2a). The elements dimensions were up to 2.5 cm×2.5 cm for the top and bottom chord of the truss and about 1.5 cm×1.5 cm for the diagonals. The rigid elements were modeled for welded connections between the diagonals and chords. In this model, structural eccentricities taken from the design project were preserved. About 480 spatial frame elements (with six degrees of freedom at the node) were used to build the beam model of the structure. In this case, the separated members of the truss (diagonals, chords) were joined axially at the nodes. Each element between the nodes was divided to ten parts (Fig. 2b).

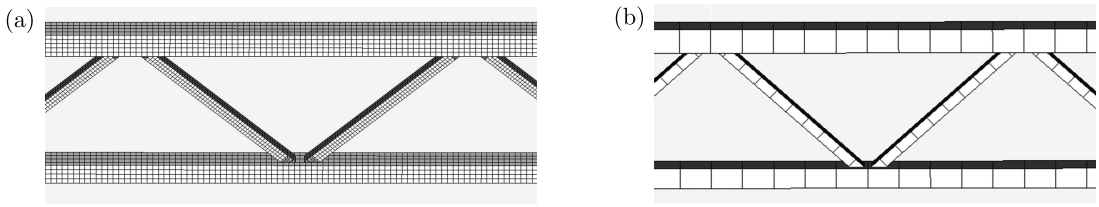

Fig. 2. The numerical models: (a) shell model, (b) beam model

The elastic braces were modeled by means of *Dof-spring* elements with translational and rotational (out of the truss plane) stiffness. In the shell model, these elements were situated at the top shelf of the top chord. In the beam model the elements were connected to the selected nodes located at the center of gravity of the top chord. In both cases (beam and shell models) the truss was loaded by concentrated forces located at the braced joints (gravity loading). The bi-linear elasto-plastic material model was implemented to conduct nonlinear analysis ($E = 210\,\text{GPa}$, $\nu = 0.3$, $f_y = 275\,\text{MPa}$). Numerical research was performed for the structure with a constant stiffness distribution along the top chord length and also for the parabolic stiffness distribution (Fig. 3, Eqs. (2.1) and (2.2))

$$K(x) = k \tag{2.1}$$

where: $K(x)$ – function to describe the distribution of brace stiffness along the truss length, k – brace stiffness (translational), x – distance from the pinned (marginal) support to the elastic support at the top chord (brace)

$$K(x) = \frac{1}{\delta(x)} \tag{2.2}$$

where $\delta(x)$ – function to describe flexibility of the bracing system.

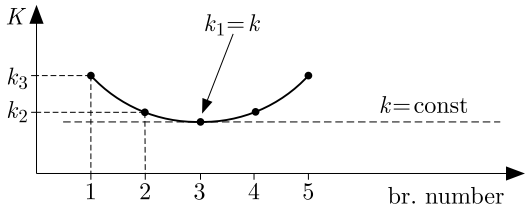

Fig. 3. The distribution of the brace translational stiffness along the truss length

In the second case, the brace stiffness was calculated due to on account of flexibility presented in Eq. (2.3). Based on those calculations the stiffness of braces No. 2 and 4 (k_2) was 12.5% higher, and for braces No. 1 and 5 (k_3) 80% higher in comparison to brace stiffness No. 3 (k_1) located in the middle of the span (Fig. 1)

$$\delta(x) = \frac{-4\delta_o}{L^2}x^2 + \frac{4\delta_o}{L}x \tag{2.3}$$

where: δ_o – flexibility of the brace system at the middle of the span, L – truss length.

3. Stability and load bearing capacity of the structure

A linear buckling analysis was made for the shell and beam models of the truss. Based on the numerical results one can conclude that the buckling load was dependent on the stiffness of side elastic supports (Fig. 4). In each case, the loading magnitude raised due to an increase in braces translational or rotational stiffness. However, it was observed that there was a threshold (minimum) brace stiffness above which the increase of buckling load was small (less than 10%). For the truss supported by elastic braces of stiffness $k = 650\,\mathrm{kN/m}$ (shell model), the magnitude of buckling load was about 10% lower in comparison to the structure with rigid braces $k = 10^6\,\mathrm{kN/m}$, $k_{rot} = 0\,\mathrm{kNm/deg}$. The same loading magnitude $P_{cr} = 267\,\mathrm{kN}$ was reached for the truss with elastic braces of stiffness equal to $k = 590\,\mathrm{kN/m}$ and $k_{rot} = 5\,\mathrm{kNm/deg}$ or $k = 540\,\mathrm{kN/m}$ and $k_{rot} = 10^6\,\mathrm{kNm/deg}$. In each case (for the beam and shell models of the structure), the above described threshold (translational brace stiffness) decreased as a result of taking into account the rotational stiffness (for the same loading level). A further decrease in the threshold stiffness was noticed if the constant brace stiffness k was replaced by a parabolic stiffness distribution k_1, k_2, k_3.

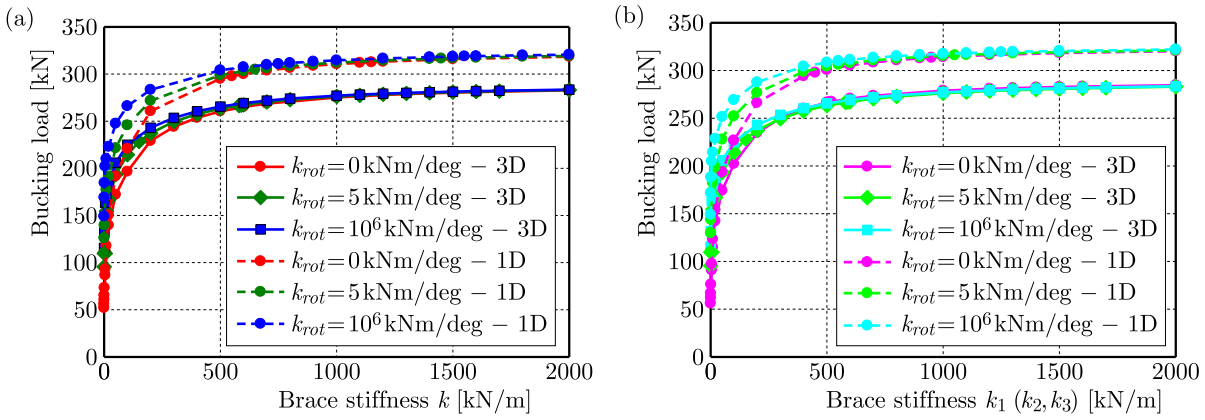

Fig. 4. The relation between the buckling load for the truss (beam and shell models) and brace translational stiffness for: (a) constant brace stiffness k, (b) parabolic brace stiffness distribution k_1, k_2, k_3, with respect to the brace rotational stiffness k_{rot}

In each case, the buckling load raised when the rotational brace stiffness was added. However, this influence decreased due to the rise of brace translational stiffness. The loading magnitudes obtained for the truss supported by braces of constant stiffness k or parabolic stiffness distribution k_1, k_2, k_3 were comparable. In that case, the differences were up to 5%.

The buckling loads obtained for the beam models were up to 15% higher than for the shell models. The reason for these discrepancies were differences in the modeling method described in the previous Section. The buckling modes for selected braced structures are presented on Fig. 5.

A static nonlinear analysis was made for the shell models of the tested structures.

In that case, a bilinear elasto-plastic steel model was implemented. The initial geometric imperfections in the form of arch curvature of the top chord (based on the PN-EN 1993-1-1, 2005 requirements) and an imperfection corresponding to the buckled shape of the truss (with rigid braces, Fig. 5c) were taken into account. The imperfection amplitude was equal to $L/500$ (the maximum displacements magnitude out of the truss plane). The analysis was carried out for the truss stiffened by elastic (translational) braces with a constant or parabolic stiffness distribution. In each case, the rotational brace stiffness equaled to $k_{rot} = 0\,\mathrm{kNm/deg}$ or $k_{rot} = 5\,\mathrm{kNm/deg}$ or $k_{rot} = 10^6\,\mathrm{kNm/rad}$.

The equilibrium paths obtained from the numerical analysis are presented in Fig. 6. In most cases, the maximum loading magnitude (limit load) depended on the elastic brace stiffness.

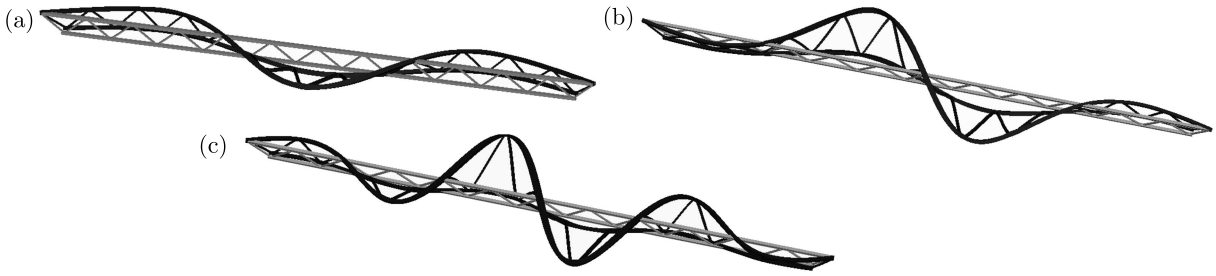

Fig. 5. Buckling modes for the truss (beam and shell models) with braces of stiffness: (a) $k = 100\,\mathrm{kN/m}$ or $k_1 = 100\,\mathrm{kN/m}$, $k_2 = 112.5\,\mathrm{kN/m}$, $k_3 = 180\,\mathrm{kN/m}$ and $k_{rot} = 0\,\mathrm{kNm/deg}$, (b) $k_1 = 100\,\mathrm{kN/m}$, $k_2 = 112.5\,\mathrm{kN/m}$, $k_3 = 180\,\mathrm{kN/m}$ and $k_{rot} = 5\,\mathrm{kNm/deg}$ or $k_{rot} = 10^6\,\mathrm{kNm/deg}$, (c) $k = 10^6\,\mathrm{kN/m}$ or $k = 10^6\,\mathrm{kN/m}$ and $k_{rot} = 10^6\,\mathrm{kNm/deg}$

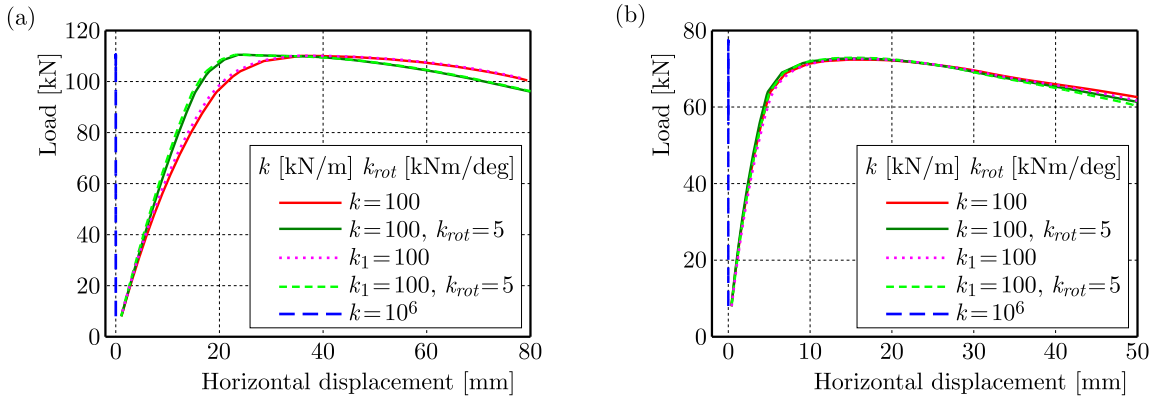

Fig. 6. The relation between truss loading and horizontal displacement of the top chord for the structure with an imperfection in the form of: (a) arch curvature (displacement in the middle of the span), (b) buckling mode (leading displacement at 3.0 m form the middle of the span)

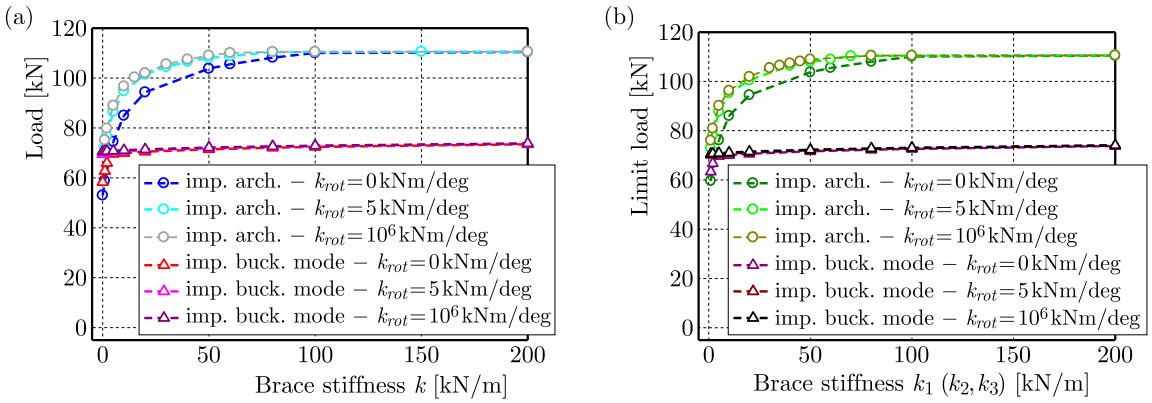

Fig. 7. The relation between the limit load and brace stiffness for the truss with: (a) constant brace stiffness distribution, (b) parabolic brace stiffness distribution, with respect to the shape of the structure initial imperfections

Similarly to the LBA results, the structure bearing capacity slightly raised (up to 2%) if the parabolic brace stiffness k_1, k_2, k_3 was taken into account in comparison to the truss with constant brace stiffness k. The out of plane truss displacements and limit load significantly depended on the shape of initial geometric imperfections. The loading capacity of the structure with an imperfection in the form of a buckling mode was up to 35% lower in comparison to the truss with the initial arch imperfection. An increase of the brace stiffness above 100 kN/m (k or k_1, k_2, k_3) had no influence on the truss limit load (differences below 1%) for the structure

with an initial imperfection shape recommended by code requirements (Fig. 7). However, it is worth noting that for the magnitude of brace stiffness mentioned above, the truss horizontal displacements were much higher (up to 34 mm in the middle of the span, at the limit state) in comparison with the truss with rigid braces (Fig. 7a). The shape of initial geometric imperfection also had a significant impact on the shape of structure deformation at the limit state (Fig. 8). Based on the results, it was observed that the plasticification range (depending on the loading level) occurred at the structural joints and also at the top and bottom chord of the truss.

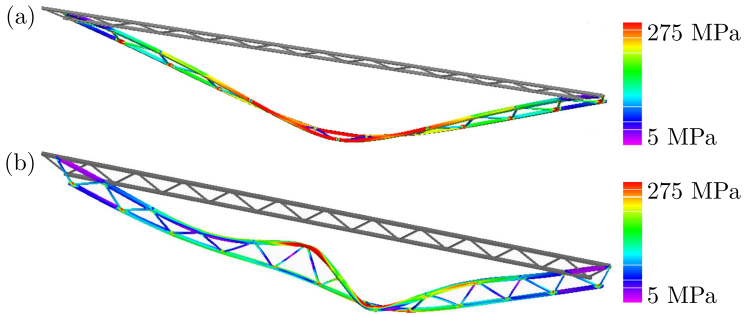

Fig. 8. The deformation and the stress state (HMH hypothesis, top surface of the shell model element) at the limit load for the braced truss $k = 100\,\mathrm{kN/m}$, $k_{rot} = 5\,\mathrm{kNm/deg}$ with an imperfection in the form of: (a) arch curvature, (b) buckling mode

4. Reactions in elastic braces

From the nonlinear analysis, reactions in elastic braces were obtained (Figs. 9-11). For the truss with the arch imperfection, the highest horizontal force was reached for the brace located in the middle of the span. However, the reaction in this brace had the smallest magnitude (absolute value) for the initial imperfection in the form of buckling mode. Based on the analysis results, one can conclude that in many cases at the limit state, the reaction in elastic braces had changeable sign. The reason was not only the brace stiffness but also the shape of the imperfection. In some cases (e.g. $k = 100\,\mathrm{kN/m}$ or $k_1 = 100\,\mathrm{kN/m}$, $k_2 = 112.5\,\mathrm{kN/m}$, $k_3 = 180\,\mathrm{kN/m}$, structure with initial arch imperfection) the braces located near the marginal supports were subjected to compression to a certain loading level. In the next loading step, the global deformation of the structure changed and the considered brace was subjected to tension. The differences in reaction forces in the loaded effort brace with a constant or parabolic stiffness distribution were up to 14%, for the arch imperfection (e.g. $k = 10\,\mathrm{kN/m}$, $k_{rot} = 0\,\mathrm{kNm/deg}$). These differences were up to 13% for the buckling mode imperfection.

The forces in elastic braces obtained from numerical analysis were compared to the stabilizing load calculated on the basis of actual code requirements (PN-EN 1993-1-1, 2005). The equivalent load was determined on the basis of Eq. (1.2). In this case, only the gravity loading was taken into consideration (Fig. 1). The influence of external (horizontal) loading was omitted $q_z = 0\,\mathrm{kN/m}$. The assumed truss loading was equal to 70 kN. That loading level was taken into account on the basis of nonlinear analysis results (GMNIA) obtained for the structure supported by braces with stiffness $k \geqslant 10\,\mathrm{kN/m}$ or $k_1 \geqslant 10\,\mathrm{kN/m}$ (initial truss imperfection in the form of buckling mode). The maximum magnitude of the normal force N_{ed} in the truss top chord was taken into account (from the middle of the span). The results for the structure with elastic braces with stiffness $k = 100\,\mathrm{kN/m}$ were presented in Fig. 12. It can be observed that the stabilizing force equal to $R_d = 0.85\,\mathrm{kN}$ (based on Eq. (1.2) and code requirements) was in most cases lower than the reactions in most loaded braces. For the structure with the initial arch imperfection, the differences between R_d and horizontal force in the elastic brace located in the middle of the span were up to 30%. Moreover, it should be point out that the equivalent load determined on

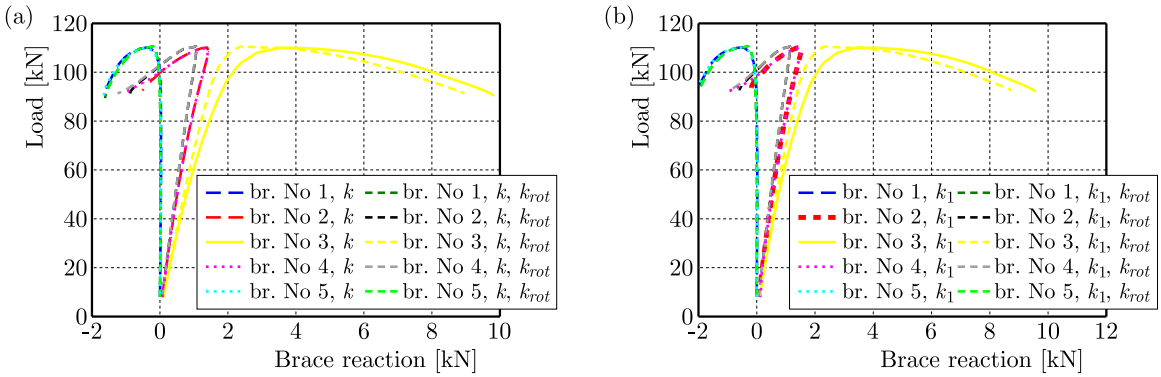

Fig. 9. The relation between the truss loading and reactions in elastic braces (initial imperfection-arc curvature at the top chord): (a) constant brace stiffness distribution $k = 100\,\mathrm{kN/m}$ ($k_{rot} = 0\,\mathrm{kNm/deg}$ or $k_{rot} = 5.0\,\mathrm{kNm/deg}$), (b) parabolic brace stiffness distribution $k_1 = 100\,\mathrm{kN/m}$, $k_2 = 112.5\,\mathrm{kN/m}$, $k_3 = 180\,\mathrm{kN/m}$ ($k_{rot} = 0\,\mathrm{kNm/deg}$ or $k_{rot} = 5.0\,\mathrm{kNm/deg}$)

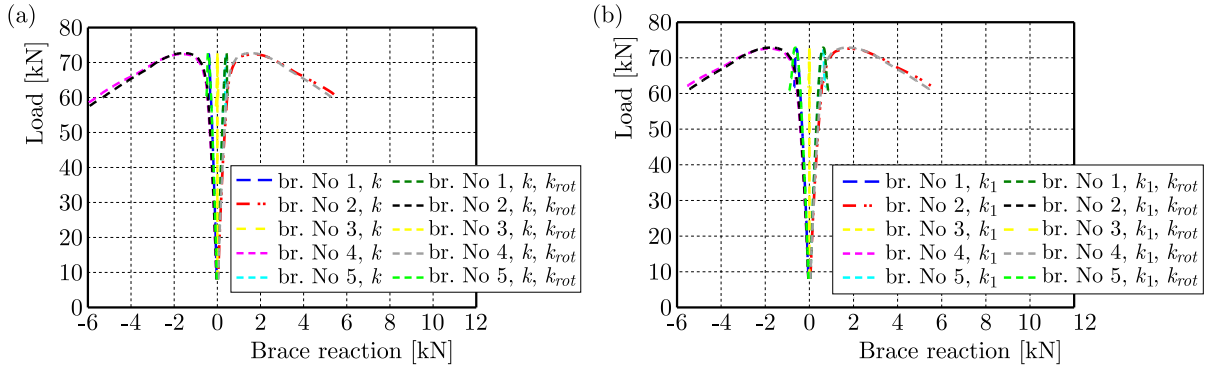

Fig. 10. The relation between the truss loading and reactions in elastic braces (initial imperfection-buckling mode): (a) constant brace stiffness distribution $k = 100\,\mathrm{kN/m}$ ($k_{rot} = 0\,\mathrm{kNm/deg}$ or $k_{rot} = 5.0\,\mathrm{kNm/deg}$), (b) parabolic brace stiffness distribution $k_1 = 100\,\mathrm{kN/m}$, $k_2 = 112.5\,\mathrm{kN/m}$, $k_3 = 180\,\mathrm{kN/m}$ ($k_{rot} = 0\,\mathrm{kNm/deg}$ or $k_{rot} = 5.0\,\mathrm{kNm/deg}$)

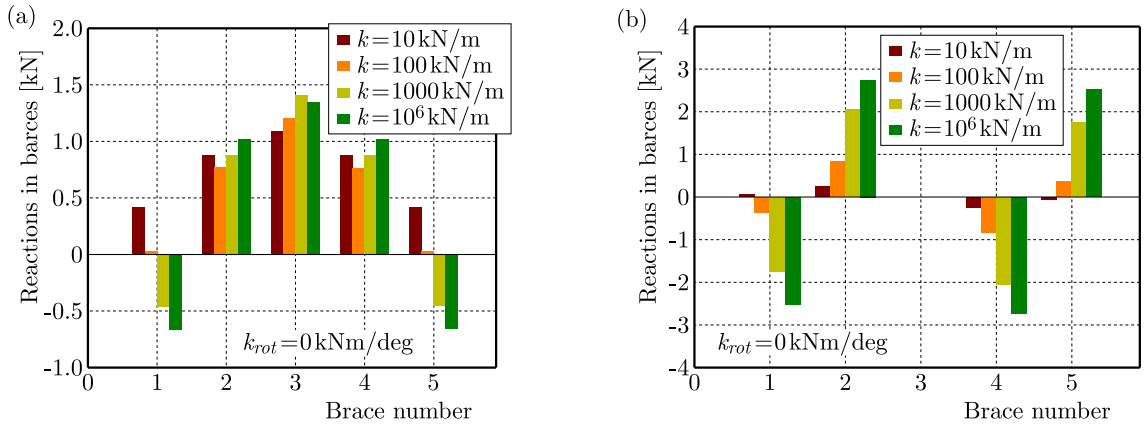

Fig. 11. The reactions in elastic supports versus the brace number for the truss with initial imperfection in the form of: (a) arch curvature of the top chord, (b) buckling mode (for selected stiffness magnitudes)

the basis of code requirements was constant (linear distribution) in opposite to GMNIA results performed for the structure with two different shapes of initial imperfections. In each case, the reactions in elastic braces (of translational stiffness) decreased due to an increase in rotational brace stiffness.

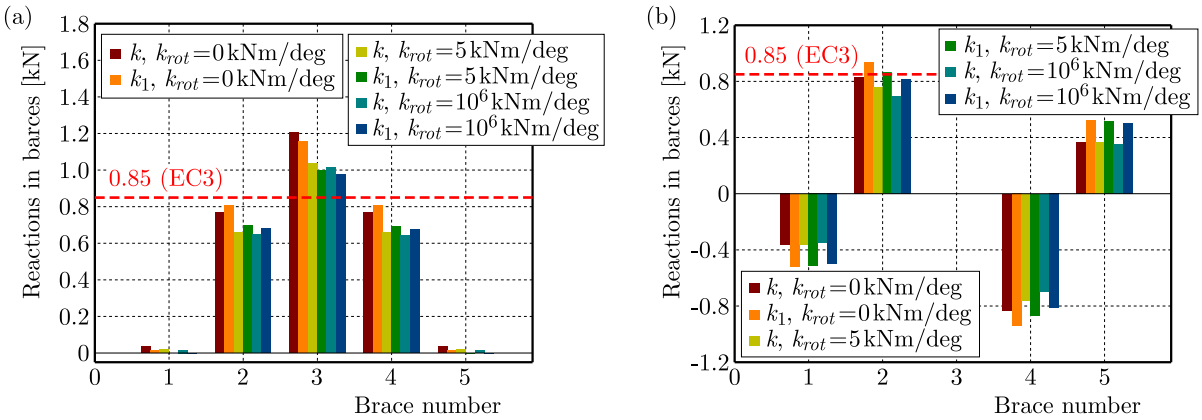

Fig. 12. The reactions in elastic supports versus the brace number for the truss with initial imperfection in the form of: (a) arch curvature of the top chord, (b) buckling mode for $k = 100\,\mathrm{kN/m}$ or $k_1 = 100\,\mathrm{kN/m}$, $k_2 = 112.5\,\mathrm{kN/m}$, $k_3 = 180\,\mathrm{kN/m}$ ($k_{rot} = 0\,\mathrm{kNm/deg}$ or $k_{rot} = 5.0\,\mathrm{kNm/deg}$ or $k_{rot} = 10^6\,\mathrm{kNm/deg}$)

In the present studies, the reactions in braces were obtained from nonlinear analysis made for the imperfect truss model. Based on code recommendations (PN-EN 1993-1-1, 2005), the global imperfections (for the building) and local imperfections (for the element) should be taken into account in the design process. In the research, two different shapes of assumed geometric imperfections were considered. In each case, the maximum imperfection amplitude (horizontal displacements out of the truss plane) was equal to $L/500$ (based on the PN-EN 1993-1-1, 2005, for single element to be braced). However, it is worth noting that the imperfection amplitude can also be assumed on the basis of standards referred to the steel section products. These codes contain detailed information on permissible deviations in terms of shape of the cross-section and element straightness. Moreover, the manufacturing accuracy of the structure production presented in (PN-EN 1090-1, PN-EN 1090-2) can be treated as the guideline for the imperfection modeling. A combination of different shapes of the imperfections which was not considered in the present paper may also influence the structure capacity (Lindgaard *et al.*, 2010). Based on real structure measurements (Šmak and Straka, 2012), the shape and amplitude of the truss initial geometric imperfections had a significant impact on the distribution of loads in the bracing system.

5. Conclusions

Based on the conducted research, the following conclusions can be formulated:

- An increase of elastic brace stiffness above the threshold stiffness did not result in a significant increase of the buckling load or limit load.
- The limit load for the structure with initial imperfection in the form of arch curvature (the shape based on actual code requirements) supported by rigid braces was about 29% higher in comparison to the truss with buckling mode imperfection.
- Based on the GMNIA results, the parabolic brace stiffness distribution (along the truss length) caused that the truss capacity raised only about 2% in comparison to the structure supported by braces with constant stiffness. In that case, the differences between reactions in most loaded elastic supports were up to 14%.
- The stabilizing load determined on the basis of actual code requirements was linear and could be characterized by constant intensity. In that case, the variable normal force distribution along the compressed element length (truss top chord) should be taken into account.

In the shell model of the truss, the distribution of reactions in elastic braces was in each case non-uniform. In many cases the reactions had changeable sign due to brace stiffness and shape of the initial geometric imperfection.

- Mostly, the reactions in greatly loaded braces were higher than stabilizing forces given by code requirements. The differences were up to 30%
- An increase of brace rotational stiffness caused a decrease in elastic brace reactions (horizontal forces).

The present research was limited to analysis of a single truss with precisely defined geometry, boundary and loading conditions. However, based on the experimental test results presented in literature (Jankowska-Sandberg and Kołodziej, 2013; Piątkowski, 2021; Krajewski, 2021) performed for different types of flat trusses, the impact of brace stiffness (translational) on the structure capacity was confirmed. In this case, steel trusses characterized by different cross-section shapes (closed or built-up) and geometric dimensions, marginal and intermediate (elastic) supports were taken into consideration. Nevertheless, the real structural connection details between the top chord and the brace (gusset planes, screws etc.) were not taken into account neither in the presented parametric studies nor in the experimental tests mentioned above. The stability analysis of the trusses updated by numerical modeling of connection details and also by experimental tests including real imperfection measurements are the next research step.

Acknowledgement

A part of the research was carried out within the grant 2022/06/X/ST8/00656 National Science Centre, Poland, Miniatura "Influence of the rotational stiffness of the connection between the brace and the chord on the stability of lattice roof trusses subjected to wind loading – experimental tests and numerical analysis".

References

1. Biegus A., 2015, Trapezoidal sheet as a bracing preventing flat trusses from out-of-plane buckling, *Archives of Civil and Mechanical Engineering*, **15**, 3, 735-741
2. Biegus A., Czepiżak D., 2018, Generalized model of imperfection forces for design of transverse roof bracings and purlins, *Archives of Civil and Mechanical Engineering*, **18**, 267-279
3. Biegus A., Czepiżak D., 2019, Equivalent stabilizing force of members parabolically compressed by longitudal variable axial force, *Matec Web of Conferences*, **262**
4. Czepiżak D., 2013, The simplified method for calculation of roof cross braces (in Polish), *Engineering and Construction*, 598-600
5. Czepiżak D., Biegus A., 2016, Refined calculation of lateral bracing system due to global geometrical imperfections, *Journal of Constructional Steel Research*, **119**, 30-38
6. Femap with NX Nastran, Instruction manual, Siemens Product Lifecycle Management Software INC., 2009
7. Iwicki P., 2007, Stability of trusses with linear elastic side-supports, *Thin Walled Structures*, **45**, 849-854
8. Iwicki P., 2010, Sensitivity analysis of critical forces of trusses with side bracing, *Journal of Constructional Steel Research*, **66**, 923-930
9. Jankowska-Sandberg J., Kołodziej J., 2013, Experimental study of steel truss lateral-torsional buckling, *Engineering Structures*, **46**, 165-172
10. Krajewski M., 2021, Stability of trusses with elastic side supports, PhD. thesis, Gdansk University of Technology

11. Krajewski M., Iwicki P., 2016, Stability of an imperfect truss loaded by wind, *Engineering Transactions*, **64**, 4, 509-516

12. Lindgaard E., Lund E., Rasmussen K., 2010, Nonlinear buckling optimization of composite structures considering "worst" shape imperfections, *International Journal of Solids and Structures*, **47**, 3186-3202

13. Piątkowski M., 2021, Experimental research on load of transversal roof bracing due to geometrical imperfections of truss, *Engineering Structures*, **242**, 112558

14. PN-EN 1993-1-1, 2005, Eurocode 3: Design of steel structures – Part 1-1: General rules and rules for buildings

15. PN-EN 1090-1+A1:2012 Execution of steel structures and aluminum structures – Part 1: Requirements for conformity assessment of structural components

16. PN-EN 1090-2, 2018, Construction of steel and aluminum structures. Part 2: Technical requirements regarding steel structures

17. Šmak M., Straka B., 2012, Geometrical and structural imperfections of steel member systems, *Procedia Engineering*, **40**, 434-439

Manuscript received October 30, 2023; accepted for print January 19, 2024